

# We are IntechOpen, the world's leading publisher of Open Access books Built by scientists, for scientists

**4,800**

Open access books available

**122,000**

International authors and editors

**135M**

Downloads

Our authors are among the

**154**

Countries delivered to

**TOP 1%**

most cited scientists

**12.2%**

Contributors from top 500 universities



**WEB OF SCIENCE™**

Selection of our books indexed in the Book Citation Index  
in Web of Science™ Core Collection (BKCI)

Interested in publishing with us?  
Contact [book.department@intechopen.com](mailto:book.department@intechopen.com)

Numbers displayed above are based on latest data collected.

For more information visit [www.intechopen.com](http://www.intechopen.com)



# Preoperative Estimation and Resection of Gliomas Using Positron Emission Tomography/Computed Tomography Neuronavigation

Yang Shuyuan<sup>1,2</sup>, Zhang Chuan<sup>1</sup>, Yue Shuyuan<sup>1</sup>,  
Cai Li<sup>3</sup>, Gao Shuo<sup>3</sup> and Zhu Tao<sup>1</sup>

<sup>1</sup>Department of Neurosurgery, Tianjin Medical University General Hospital

<sup>2</sup>Tianjin Neurological Institute; Key Laboratory of Post-trauma Neuro-repair and  
Regeneration in Variations and Regeneration of Nervous System

<sup>3</sup>PET-CT Center, Tianjin Medical University General Hospital

P.R. China

## 1. Introduction

Gliomas are the most common primary neoplasm of the brain, and their treatment presents a number of challenging diagnostic and therapeutic problems for neuro-oncologists. The outcomes for patients with glioma can be quite variable, and there is no consensus regarding the best treatment. To this point, the most widely accepted treatment has been surgical excision, followed by radiotherapy and chemotherapy. Gliomas, however, tend to be diffuse, with ill-defined borders, particularly in grade II and a part of grade III tumors, making them difficult to distinguish from normal or edematous brain tissue during the excision. The percentage of gliomas that are completely removed through surgical intervention is disappointingly low, and this generally leads to a poor prognosis. However, cases where the glioma has been completely removed show a significant improvement in long-term prognosis compared to cases where the glioma was only partially removed. Although complete excision might be an unrealistic goal at this time, these findings suggest that even just increasing the amount of tumor excised has potential prolonging patient survival.

In glioma surgery, precise histological diagnosis during the initial operation is crucial since treatment strategies and prognosis can differ greatly depending on the histological grade. Gliomas diffusely infiltrate neighboring brain structures and are characterized by regional variations of histological malignancy [1]. Therefore, detection of the highly malignant region and delineation of the extent of the tumor are critical during preoperative evaluation.

Recently, positron emission tomography (PET) has been used for evaluation of glioma metabolism. The representative radiolabeled tracers are <sup>18</sup>F-fluorodeoxyglucose (FDG) and <sup>11</sup>C-methionine (MET). Methionine is an endogenous, essential amino acid and enters tumor cells via the L-amino acid transporter to meet the demands of accelerated protein and RNA synthesis. MET is widely used because less of the amino acid tracer is taken up by healthy brain tissue, which results in greater contrast between tumor and normal brain

tissue than what can be seen with FDG PET [2]. MET PET has been reported to delineate both benign and malignant gliomas more accurately than computed tomography (CT) or magnetic resonance imaging (MRI) [3, 4], and has been used in the diagnosis and follow-up of glioma patients [5-6]. On the other hand, malignant tumors are well known to have higher rates of glucose utilization and glycolysis, which would argue for the use of FDG PET. Several reports have demonstrated that FDG uptake in gliomas is highly correlated with the degree of malignancy [7-12]. FDG PET is ill-suited for the detection of gliomas, however, because the rate of glucose utilization of normal brain cortex is relatively high [13-15], so that when a hypermetabolic lesion is near the cortical or subcortical gray matter, it is often difficult to differentiate between tumor and normal tissue [16]. In addition, FDG uptake is known to be non-specific: high FDG accumulation has been observed in inflammatory cells and granulation tissue as well as in viable cancer cells [17-18].

Neuronavigation can precisely locate intracranial lesions and track these targets dynamically, facilitating a more complete removal of the tumor. A comprehensive survey showed neuronavigation-guided surgery of 52 primary glioblastomas achieved complete tumor resection in 31% of cases, versus 19% in a series of conventional operations [19]. These data demonstrate that neuronavigation can increase resection of glioblastoma without prolonging operating time, and increase survival time. However, computed tomography (CT) and magnetic resonance (MR) imaging cannot show the border of glioma accurately because of the tumor biological characteristics. PET shows the metabolic characteristics of tissue, which has a unique advantage in the operation of glioma using neuronavigation.

## 2. Method and clinical data

### 2.1 Patients

From May 2004 to May 2010, a total of 71 patients with gliomas received PET/CT with FDG and MET. There were 44 males and 27 females, all between the ages of 6 to 72 years old (mean  $41.7 \pm 17.2$ ). The most common presenting symptoms included headache, nausea, vomiting, seizures, hemiparesis/aphasia, and cognitive dysfunction, etc. All patients were treated surgically, and diagnosis was confirmed by pathology.

### 2.2 MRI and CT

All patients underwent brain CT, plain MRI, and enhanced MRI scans.

MRI studies were performed using a 1.5-tesla MRI system (1.5T Signa Twin-speed, infinity with Excite I; GE Medical Systems, Milwaukee, Wisconsin, U.S.A.), or a 3.0-tesla MRI system (Signa Excite HD 3.0T; GE Medical Systems) within 1 month before PET/CT imaging. The conventional imaging protocol consisted of fluid-attenuated inversion recovery sequence T1-weighted imaging (repetition time [TR] 2025 msec, echo time [TE] 8.4 msec, inversion time 750 msec, slice thickness 6.0 mm, slice gap 1.5 mm, field of view 24x18 cm, matrix 320x224, number of excitations [NEX] 2), fast-recovery fast spin-echo sequence T2-weighted imaging (TR 4000 msec, TE 110 msec, slice thickness 3.0 mm, no slice gap, field of view 24x24 cm, matrix 512x512, NEX 2), spin-echo echo-planar imaging sequence diffusion-weighted imaging (TR 10,000 msec, TE 80.1 msec, slice thickness 3.0 mm, no slice gap 1.5 mm, field of view 24x24 cm, matrix 128x128, NEX 1), and spin-echo sequence T1-weighted imaging (TR 500 msec, TE 8.4 msec, flip angle 75, slice thickness 3.0 mm, no slice gap, field of view 24x24 cm, matrix 256x150, NEX 1) 2 minutes after injection of gadolinium-diethylenetriaminepenta-acetic acid (0.1 mmol/kg). We used non-contrast-enhanced transaxial T1-weighted images (T1WI) and T2-weighted images (T2WI) for image fusion.

### **2.3 PET/CT**

<sup>18</sup>F-fluorodeoxyglucose (FDG) and <sup>11</sup>C-methionine (MET) were produced in a MINITrace cyclotron, with TRACERlab MXFDG and TRACERlab FXc synthesizer (GE Medical Systems, Milwaukee, Wisconsin, U.S.A.). PET/CT was performed using a Discovery LS PET/CT unit (GE Medical Systems, Milwaukee, Wisconsin, U.S.A.). Patients fasted for at least 6 hours prior to the PET/CT examination. A dose of 222-370 MBq (6-10 mCi) FDG and/or 555-740 MBq (15-20 mCi) MET was injected intravenously within 1 minute. Static emission scanning was performed at least 40 minutes after FDG injection or at least 20 minutes after MET injection. PET was performed in three-dimensional (3D) mode (field of view 15 cm, slice thickness 5.0 mm, slice gap 4.25 mm, matrix 128x128). The lamellar CT protocol was slice thickness 2.5 mm, slice gap 0, and matrix 512x512. Six reference markers were fixed to the scalp around the tumor before the PET/CT investigation.

### **2.4 PET/CT diagnosis**

Visual analysis: PET/CT scans of the glioma were referenced to MRI images of the lesion, and the uptake of imaging reagents was classified. Uptake lower than or close to white matter uptake was defined as low metabolism; uptake higher than white matter uptake but significantly lower than gray matter uptake was defined as moderate metabolism; and uptake near, equal to or higher than gray matter uptake was defined as high metabolism. In addition to reagent concentration within the lesion, the analysis also included reagent distribution, lesion shape, uniform or not and whether the boundary clearly.

Semi-quantitative analysis: the center region with highest reagent concentration was marked, avoiding necrotic cystic areas, to outline regions of interest (ROI). Tumor standard uptake values (SUV) were derived, and the ratios of the tumor-to-contralateral white matter (T/WM) and tumor-to-contralateral gray cortex (T/GM) were calculated.

### **2.5 PET-assisted neuronavigation glioma surgery**

Intraoperative neuronavigation was performed using a VectorVision®2 system (Brain LAB AG, Heimstetten, Germany). PET, CT, and MRI data were input into the project graphic workstation, the markers were identified, and the 3D images were rebuilt. The 3D PET image was then coregistered automatically with the 3D MRI or CT image using the registration program of the project system, and the fused image adjusted manually.

Patients were anesthetized, and their heads were fixed in a Mayfield head frame. The operative project data were input into the neuronavigation workstation, and the markers were registered with an error of  $\pm 1.5$  mm. The tumor resection was then carried out, directed by the neuronavigation system. The extent of the operative target was confirmed using the neuronavigation system.

## **3. Pathologic examination**

### **3.1 HE staining**

Sections taken from each operation specimen were fixed with formalin, embedded in paraffin, and stained with hematoxylin and eosin. The histological diagnosis was determined by an experienced neuropathologist according to the WHO classification of tumors of the central nervous system.

### 3.2 Ki-67 LI

Proliferative activity was measured by obtaining the Ki-67 proliferation index by histochemical staining of pathological specimens. Paraffin-embedded tumor specimens were recut into 3–4  $\mu$ m serial sections. Immunohistochemical staining was carried out on sections using monoclonal murine antibody MIB-1, an antibody to Ki-67 (1/100 dilution; DAKO Corp.). MIB-1 recognizes the Ki-67 antigen, a 345- and 395-kDa nuclear protein common to proliferating human cells (21). Sections were then incubated in secondary antibody for 30 min at 25°C, incubated with streptavidin peroxidase, and then washed in phosphate-buffered saline. 3,3-Diaminobenzidine tetrahydrochloride was used as a substitute substrate-chromogen solution, and sections were counterstained with Meyer's haematoxylin. For negative controls, tissue sections were incubated with mouse IgG instead of anti-Ki-67 nuclear antigen antibody. After cell staining, fields were selected randomly for cell counting. Serial sections were reviewed by an experienced neuropathologist. A minimum of 1,000 cells were counted per tissue section. All cells with nuclei staining of any intensity were defined as positive. The Ki-67 score (%) (Ki-67 LI) was defined as the percentage of cells that stained positively for Ki-67 nuclear antigen. The proliferative activity score, quantified as the percentage of MIB-1 stained nuclei per total nuclei in the sample, was estimated from a representative slide selected by the neuropathologist.

## 4. Results

### 4.1 Patient and tumor characteristics

12 cases had resections guided by PET-neuronavigation, including 2 cases of fibrous astrocytoma, 2 cases of mixed oligodendro-astrocytoma, 3 cases of anaplastic astrocytoma, 1 case of anaplastic oligodendroglioma, 1 case of anaplastic oligodendro-astrocytoma and 3 cases of glioblastoma. For heterogeneous areas of MET and FDG metabolism, specimens from the hot spots of MET and FDG uptake were resected separately with navigation, and sent to pathology.

### 4.2 PET visual analysis

FDG PET examination: 38 of the patients in the study had high-grade gliomas (grade III, or IV). Visual analysis revealed high metabolic lesions with clear boundary in 36 of the 38 cases. FDG distribution within the lesion area was uneven; cystic and necrotic areas were defect for reagent, and the edematous area around the tumor showed reduced metabolism. In the remaining 3 high-grade cases (1 medulloblastoma and 2 anaplastic astrocytomas) visual analysis revealed moderate metabolism. 33 of the patients in the study had low-grade gliomas (grade I, or II). In 31 of the 33 cases, visual analysis revealed either moderate or low metabolic lesions, and FDG distribution was relatively homogeneous. However, when the tumor was located within the gray/white matter junction, the high metabolism of surrounding normal gray matter often made it difficult to distinguish the lesion boundaries. The remaining 2 low-grade cases (both oligodendrogliomas) displayed high metabolism. FDG PET visualization results were concordant with pathological grading in 66 of the 71 cases (coincidence rate= 93%).

MET PET examination: Visual analysis revealed high metabolism in 66 of the 71 cases. Visual analysis of the remaining 5 cases (all grade II fibrous astrocytomas) revealed low metabolism. However, compared with FDG, MET uptake in normal brain tissue has very low background, which can provide a better contrast to scope the tumor border, and helpful to detect the low-grade glioma. In some cases, FDG and MET were inconsistent at the concentrated area.

Characteristic	No. of cases
Age (yrs)	
6-72 (average 41.7±17.2)	71
Sex	
Female	44
Male	27
WHO classification	
Grade I	8
pilocytic astrocytoma	3
dysembryoplastic neuroepithelial tumor	3
subependymal giant cellular astrocytoma	1
ganglion cellular glioma	1
Grade II	25
Astrocytoma	12
Oligodendroglioma	5
Oligodendro - astrocytoma	8
Grade III	21
Anaplastic astrocytoma	14
Anaplastic oligodendroglioma	3
Anaplastic oligoastrocytoma	4
Grade IV	17
Glioblastoma	14
medulloblastoma	2
PNET	1

Table 1. Patients and tumor characteristics

#### 4.3 PET semi-quantitative analysis and Ki-67 LI

PET semi-quantitative analysis: the centre region with highest reagent concentration was marked, avoiding necrotic cystic area, to outline regions of interest (ROI), derived tumor standard uptake value (SUV); then calculate the ratios of the tumor / contralateral white



matter (T / WM) and tumor / contralateral gray cortex (T / GM). PET semi-quantitative indicators and Ki-67 LI results were shown in Table 2. Analysis of variance (One-Way ANOVA) for FDG: the results showed statistically significant differences between groups ( $F_{SUV} = 9.371$ ,  $F_{T/WM} = 9.907$ ,  $F_{T/GM} = 17.867$ , both  $P < 0.01$ ), between low-grade (grade I and II) gliomas and high-grade (grade III and IV) ( $P < 0.01$ ), between III and IV grade (T/GM FDG,  $P = 0.029$ ). However, various indicators did not show manifest difference between grade I and (II) ( $P > 0.05$ ). MET results displayed only T/GM MET in statistically significant difference between groups ( $F_{T/GM} = 3.026$ ,  $P = 0.048$ ), and between II and IV grade ( $P = 0.011$ ). The remaining indicators were no significant differences ( $P > 0.05$ ). Correlation analysis showed that: FDG and MET PET in three semi-quantitative indexes were positively correlated, SUV, T/WM and T/GM of the correlation coefficient  $r$  values were 0.608, 0.708, and 0.716 (all  $P < 0.001$ ). T/GM FDG and T/GM MET was positively correlated with Ki-67 LI,  $r$  were 0.610, 0.729 (all  $P < 0.001$ ).

Tumor Grade	n	SUV <sub>FDG</sub>	T/WM <sub>FDG</sub>	T/GM <sub>FDG</sub>	SUV <sub>MET</sub>	T/WM <sub>MET</sub>	T/GM <sub>MET</sub>	Ki-67 LI
WHO I	8	4.38±4.36	1.43±0.54	0.45±0.14	3.94±1.57	4.18±1.6	1.98±0.93	2.95±0.75
WHO II	25	5.02±2.68	1.57±0.62	0.58±0.21	3.58±3.29	4.13±2.28	1.91±1.07	5.35±3.98
WHO III	21	11.69±7.77	2.84±0.81	1.11±0.47	5.11±2.42	5.29±3.12	2.84±1.24	10.41±7.70
WHO IV	17	13.59±4.80	3.86±1.76	1.54±0.47	5.39±2.11	6.29±1.5	3.51±1.2	25.35±1.82

Table 2. PET semi-quantitative index and Ki-67 LI.

#### 4.4 PET and CT, MRI

For the typical grade IV glioblastoma, MRI showed the mass as hypointense on the T1-weighted images, and hyperintense on the T2-weighted images, with irregular ring enhancement accompanied by necrosis or cystic tissue. But in three of the glioblastoma cases, CT and MRI scans revealed the tumor located in the corticomedullary junction area, invading the cortex, with some slightly enhanced spots in the lesion, and peripheral edema surrounding the tumor with no clear boundary. FDG and MET PET showed irregular areas of high concentration with clear borders (especially MET). The most concentrated area of distribution inconsistent between FDG and MET in some cases, but the tumor boundary was roughly same. Under the guidance of neuronavigation, tumor samples were taken at the most concentrated FDG and MET areas respectively (Fig. 1). Pathological findings revealed: tumor cells densely located at the MET concentrated area with obvious atypical nuclei and highly proliferative vascular endothelial cell, as the typical glioblastoma grade IV character. Pathological findings for the FDG area revealed less tightly packed cells, with no obvious vascular endothelial cell proliferation, which was the junction between tumor and normal brain tissue (Fig. 2-4).

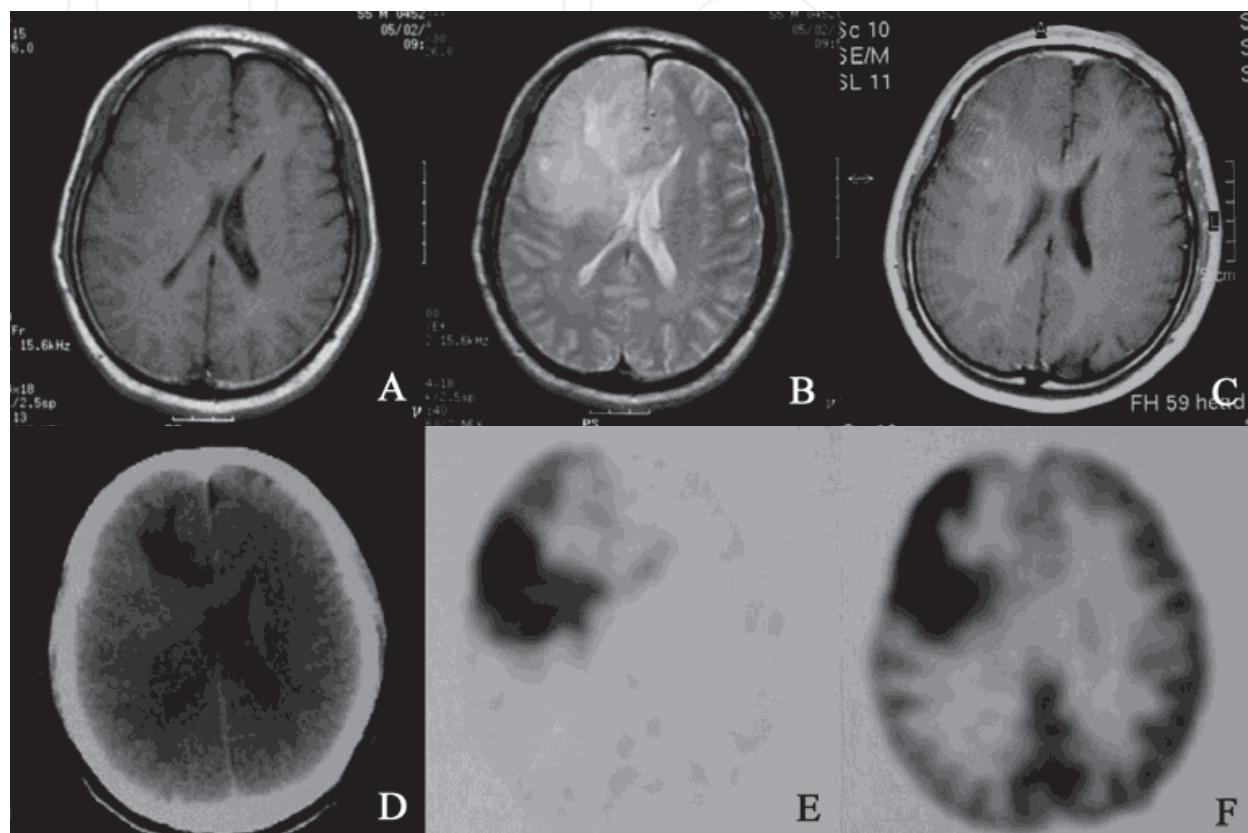


Fig. 1. A 55-year-old man with a diffuse lesion in the right frontal lobe. A-C: T1-weighted (A) and T2-weighted (B) magnetic resonance (MR) images, and T1-weighted MR image with contrast medium (C), showing a mass in the right frontal lobe with unclear margin as slightly hypointense on the T1-weighted and hyperintense on the T2-weighted images, with some slightly enhanced spots in the lesion. D: Computed tomography scan, showing the lesion as equal or slightly increased density, with an unclear border, in and below the right frontal lobe cortex. E: 11C-methionine positron emission tomography (PET) scan, showing an irregular area of high uptake with a clear border in the right frontal lobe. The area of highest MET uptake was in the posterior part of the lesion. F: 18F-fluorodeoxyglucose PET scan, showing an irregular area of high uptake which was relatively well defined in the frontal lobe. The highest FDG uptake area was in front of the MET hot area.



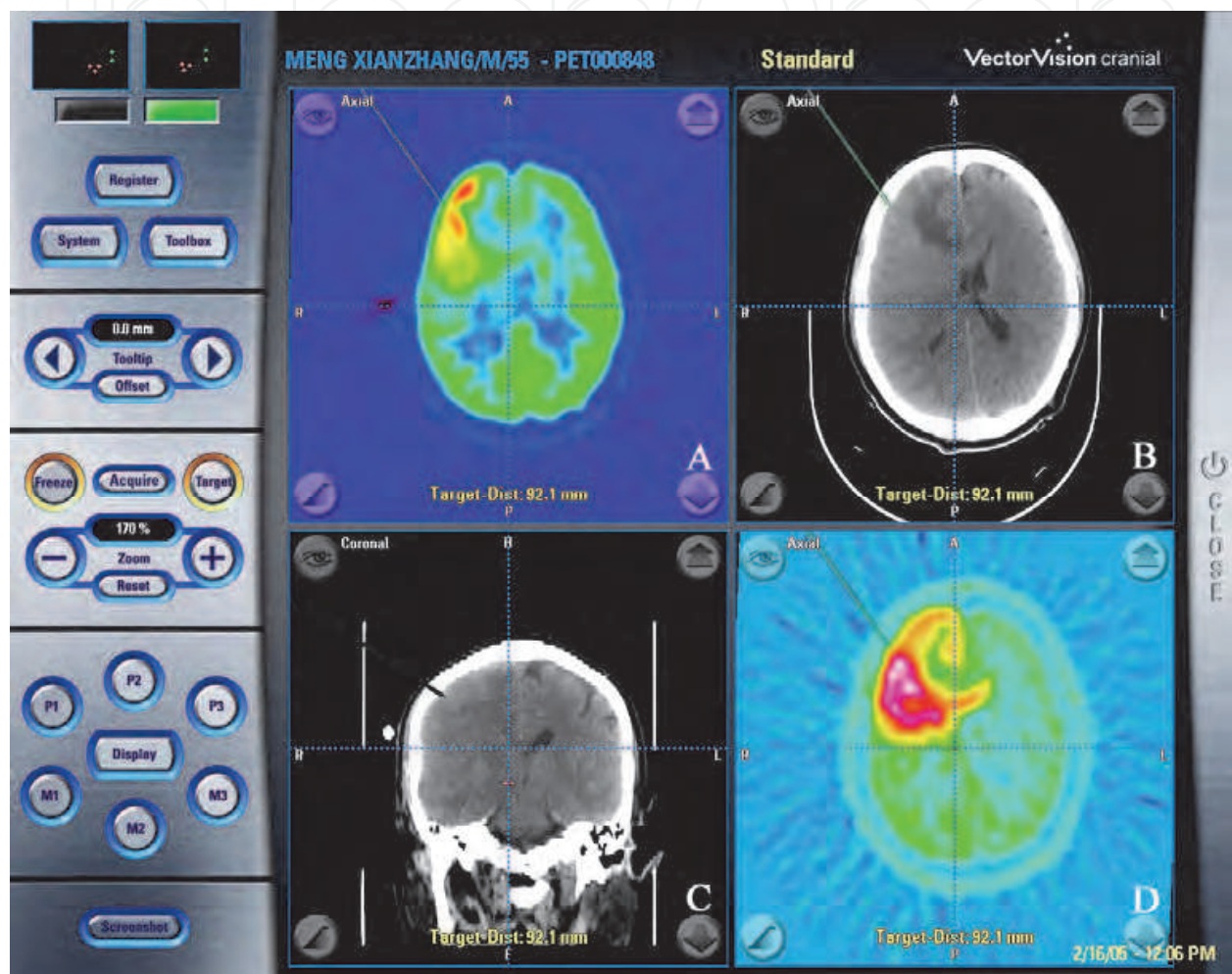


Fig. 2. Positron emission tomography (PET) neuronavigation system monitoring images captured during the operation. A: 18F-fluorodeoxyglucose PET scan; B, C: CT scans; D: 11C-methionine PET scan. CT provided the anatomic background. PET provided more distinct information of the tumor.

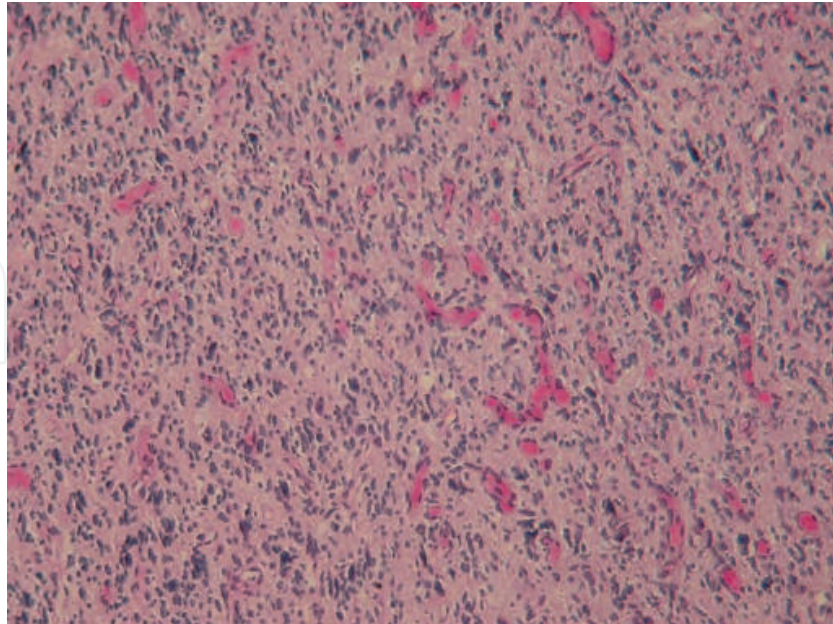


Fig. 3. Photomicrograph of the specimen resected from the hot spot demonstrated by <sup>11</sup>C-methionine positron emission tomography showing glioblastoma, World Health Organization grade 4. Nucleus deformation, and cell and vessel proliferation were prominent. Hematoxylin and eosin stain, x100.

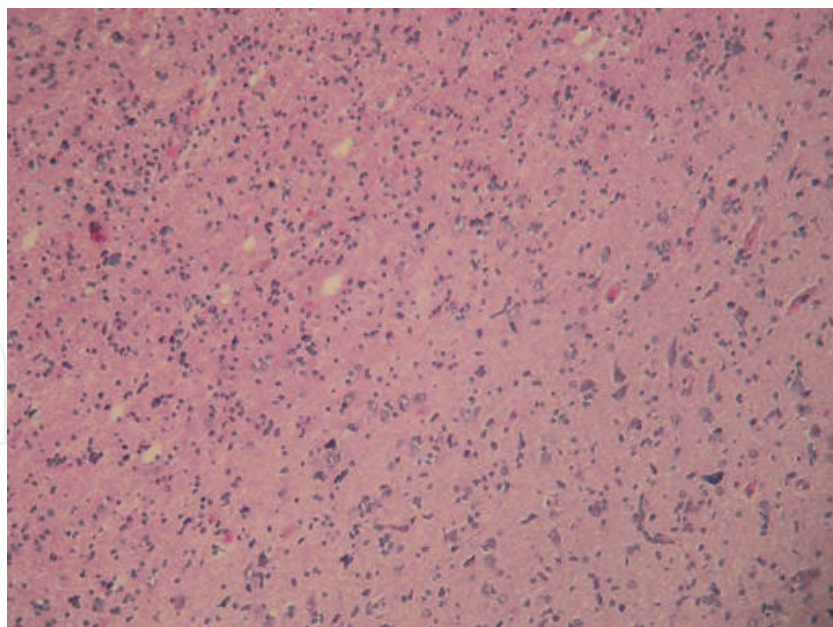


Fig. 4. Photomicrograph of the specimen resected from the hot spot demonstrated by [<sup>18</sup>F]fluorodeoxyglucose positron emission tomography showing the margin of the tumor. Nucleus deformation, and cell and vessel proliferation were similar to that of astrocytoma grade II. Hematoxylin and eosin stain, x100.



For gliomas grade II and III, MRI showed the tumor as an irregular hypointensity or an irregular hyperintensity surrounded by edema with ill-defined boundaries on the T1-weighted and T2-weighted images respectively. The lesion displayed mild enhancement or no enhancement. PET imaging, especially, MET distribution was more helpful in illustrating the tumor boundaries. Oligodendrogliomas and Oligodendroastrocytoma in particular showed the high MET concentrations (Figure 5).

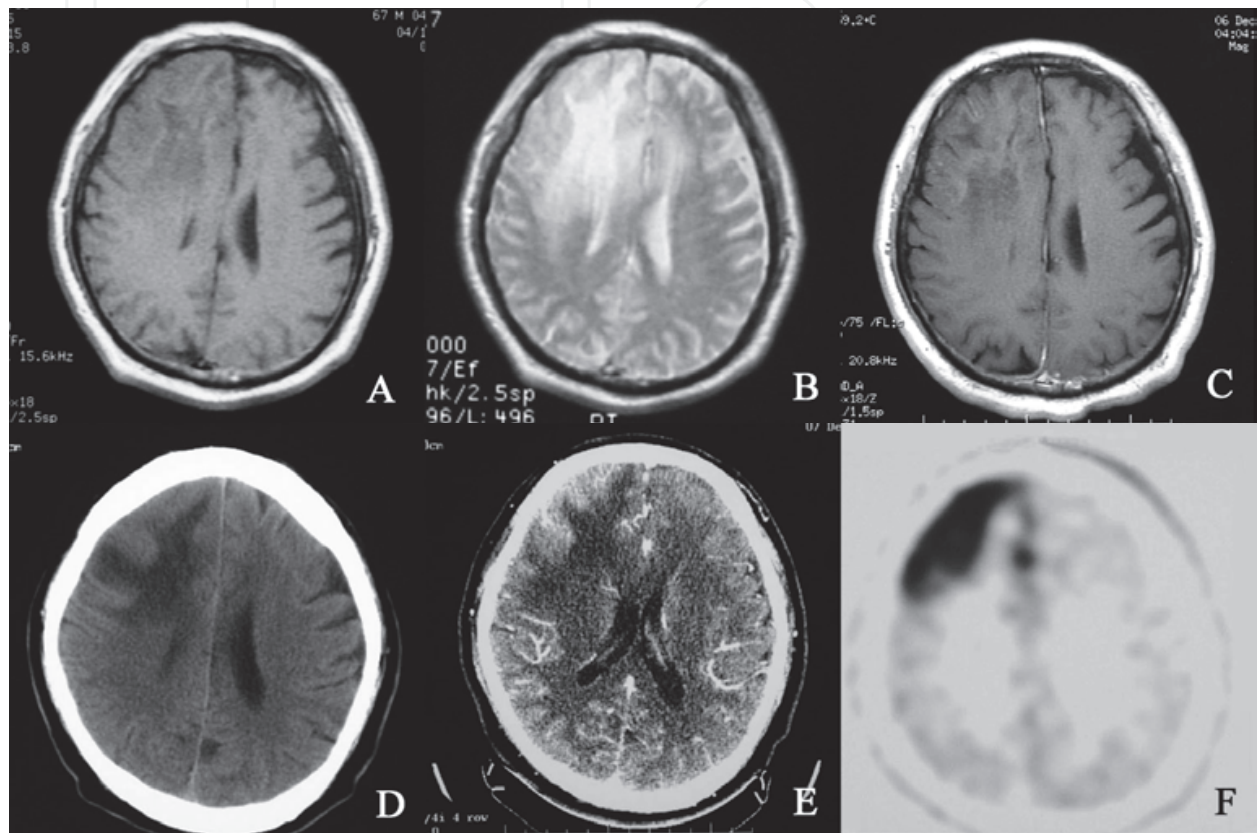


Fig. 5. A 65-year-old man with a diffuse lesion in the right frontal lobe. A-C: T1-weighted magnetic resonance images (A, B), and with contrast medium (C), showing a mass with unclear margins in the right frontal lobe, appearing as slightly hypointense on the T1-weighted and hyperintense on the T2-weighted images without obvious enhancement. D, E: Computed tomography scan (D) and with contrast medium (E), showing the irregular lesion as uniform density with an unclear border and slight enhancement deep within the right frontal lobe cortex. F: 11C-methionine positron emission tomography scan, showing an irregular high uptake area in and below the right frontal lobe cortex with a clear margin.

#### 4.5 PET neuronavigation surgery

In 4 cases of grade II gliomas, visual inspection of the surface of the brain was normal except for some localized slight gyral broadening, such that tumor location could not be determined by gross visualization. Tumor boundaries could not be clearly determined with CT and MRI scans. PET scans (especially MET), however, allowed for satisfactory delineation of the tumor boundaries. Because of this, the resections were performed using MET PET/CT neuronavigation. During the resection, the tumor tissue appeared approximately normal in color, with a slightly tenacious texture, and moderate bleeding.

After complete resection, the cross section and periphery of the tumor were checked. The cut surface appeared much like normal brain, with no necrosis or capsule (Figure 6).

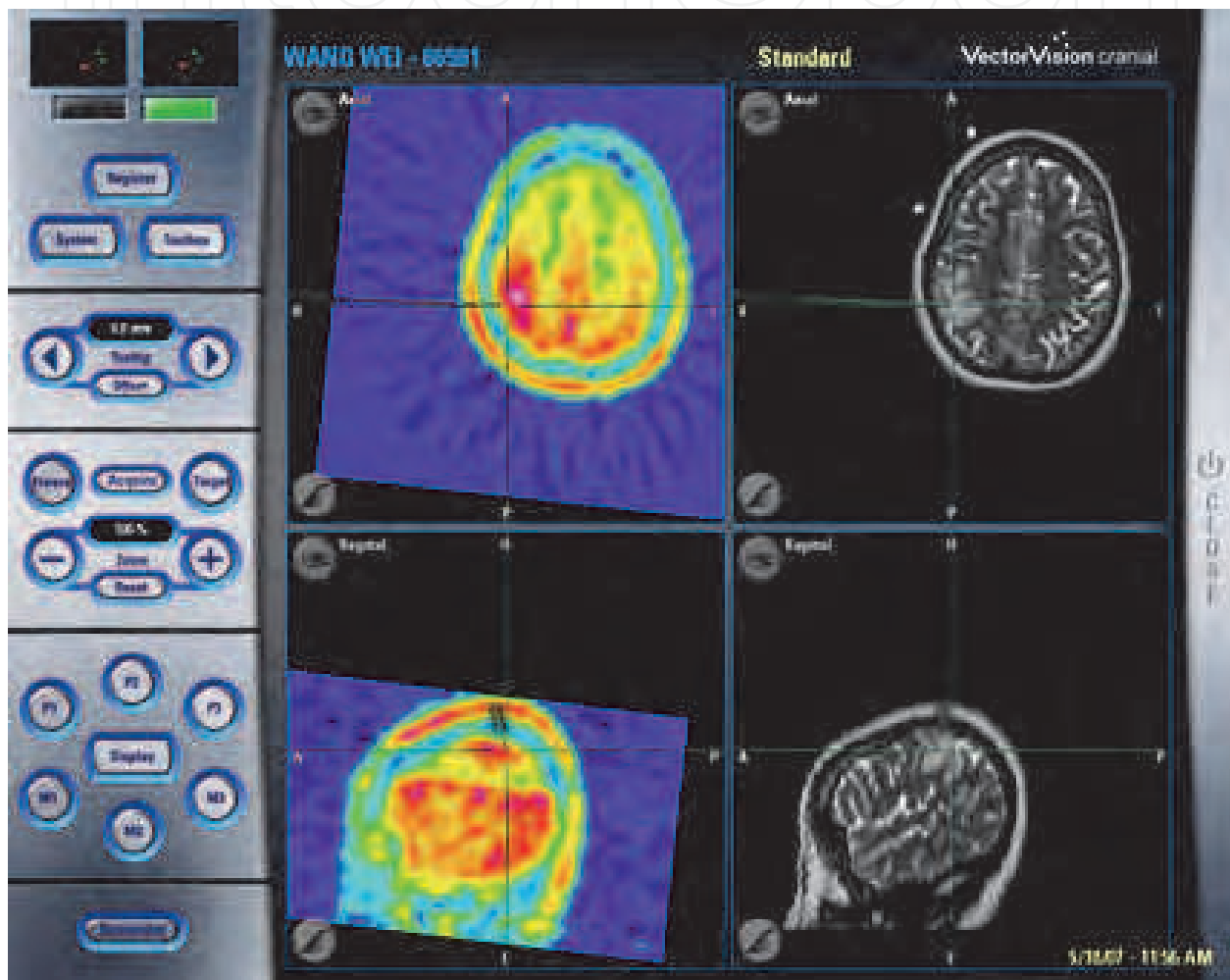


Fig. 6. Positron emission tomography (PET) neuronavigation system monitoring images captured during the operation. A 56-year-old woman with a diffuse lesion in the right frontoparietal lobe. The pathological diagnosis of the tumor is Oligodendroglioma.

Grade III and IV gliomas were characterized by abnormal color, texture and blood supply, and were all resected under the guidance of PET-assisted navigation. The specimens taken from different tracer concentrated areas were sent to pathology. Postoperative imaging demonstrated complete resection of the suspected tumor area (Figure 4).

## 5. Discussion

### 5.1 The value of PET assessment for preoperative glioma

In 1982, Di Chiro confirmed by FDG PET that a tumor's malignancy level is closely related to the tissue's glucose utilization [20]. FDG PET is widely utilized to detect malignant tumors. Increased glucose uptake is usually associated with higher malignancy and aggressiveness. In gliomas, due to high uptake in cortex and basal ganglia, and low uptake in white matter, FDG uptake showed a close relationship with histological grade or prognosis [7-12]. Patronas et al. reported that FDG uptake is a more accurate reflection of tumor grade than contrast enhancement [21], and Goldman et al. [10] proved that FDG uptake in gliomas correlated regionally with presence of anaplasia by means of FDG PET-guided stereotactic biopsy. Although FDG PET is the gold-standard detection tool for regional malignancy in gliomas, it is not perfect. In terms of delineating tumor boundaries precisely, FDG PET is obviously inferior to MET PET [2]. MET increased uptake in tumor mainly reflects the increase in amino acid trafficking activity, and indirectly represents the increase in protein synthesis. MET, however, proved better than FDG in distinguishing tumor boundaries, as the lower uptake in normal brain tissue allows for better contrast between normal and tumor tissue. In addition, fusion of MET with MRI or CT images allowed for better detection of low-grade tumors close to the cortex, smaller tumors, and tumor boundaries. Therefore, combined use of FDG and MET is reasonable in detecting regional malignancy and in delineating the extent of viable tumor tissue for preoperative evaluation of glioma surgery [22-24]. This study also found that the most concentrated area for each tracer was sometimes inconsistent in the high-grade gliomas. Comparison with pathology reports showed that MET uptake in tumor cells was more specific. [25]

Metabolic characteristics of different types of gliomas were diverse. Our and other studies found that oligodendrogliomas and oligodendroastrocytoma displayed high uptake of both MET and FDG. Oligodendrogliomas showed particularly high uptake, with MET uptake close to the level seen in anaplastic astrocytomas, and pathologically the tumor cells were highly condensed. Previous studies have demonstrated that pilocytic astrocytomas may have higher FDG and MET uptake [26]. In our study, 2 cases of pilocytic astrocytoma showed high metabolism of MET, even higher than that seen in grade II astrocytomas, but low FDG metabolism, histopathology revealed extensive capillaries. One case of subependymal giant cell astrocytoma with tuberous sclerosis showed moderate FDG uptake, and significantly elevated MET uptake, close to levels seen in glioblastomas. Pathology on this case revealed large tumor cells surrounded by a large number of expanded blood vessels. Therefore, the MET uptake of gliomas (especially low-grade gliomas) may be dependent not only on proliferative activities but also on other factors such as cerebral blood volume [27], amount of microvessels [18, 28], and cell density [29].

SUV is the most common semi-quantitative indicator, but it may be affected by many factors, such as age, blood glucose level, and medication. As such, it may not be well suited as a means for comparison across repeated examinations, and amongst different individuals.



Using the uptake ratios between the lesion and normal tissue can overcome the shortcomings. Our results show that the T/GM is of the best indicator for grading gliomas, and that FDG is better than MET in estimating a tumor's pathological character.

Recent studies have confirmed that MET uptake is closely related to the proliferation of brain tumors. During the early exponential growth phase, tumor cells can show a high degree of MET concentration. Whereas at the plateau phase MET uptake is much lower. So the level of MET uptake could be regarded as a sign of tumor cell proliferation, but it is controversial whether FDG uptake is related to cell proliferation. Our study demonstrated that uptake levels of FDG and MET in gliomas were associated with Ki-67 LI. Ki-67 LI which revealed the tumor proliferation was a prognostic indicator for cancer patients, and PET which revealed the tumor metabolic activity can also help evaluate the tumor proliferation and prognosis [30-32].

### **5.2 PET comparing with MRI and CT**

MRI and CT can display the brain organization structure clearly, and as such these are the main non-surgical methods used to initially diagnose gliomas. Currently MRI is the first choice for diagnosing tumor pathological grade and for determining the location and extent of the tumor. The malignant part of tumor is most often located in or near the area of blood-brain barrier breakdown, in which case it would appear as an area of enhancement on an MRI with medium contrast. However, T1- and T2-weighted MRI are often insufficient to definitively determine the relationship between tumor and normal or edematous tissue. This is the case with many grade II gliomas, and sometimes is seen even in grade III and IV gliomas. Furthermore, if the tumor is not located near the blood-brain barrier breakdown or the barrier has not broken down, it is near impossible to distinguish between healthy and tumor tissue, nor can the regional heterogeneity of the tumor be shown. Clinical studies have shown that gliomas often extend beyond the contrast-enhanced margin and that approximately 80% of tumor relapses occur within a 2-cm margin around the original enhanced lesion [33]. Therefore, neuronavigation using only MR imaging cannot be relied upon to outline the target completely.

In addition to CT and MR imaging, metabolic imaging with PET has been considered. PET can be used to estimate the grade and malignancy of the glioma before operation, evaluate the prognosis and the outcome of radiotherapy and chemotherapy, and show the tumor extent and heterogeneity [30, 34]. Clinical studies using radiolabeled amino acid PET, such as MET, have demonstrated superior delineation of the glioma mass compared with MRI. The use of PET over MRI allowed for differentiation between tumor and edematous tissue, and recognition of different areas of proliferation in different parts of the tumor. Confirmation of the target of stereotactic biopsy and radiotherapy by PET provides high sensitivity and specificity [35-38].

### **5.3 PET optimizing neuronavigation surgery**

Invasive growth of gliomas showed no obvious boundaries, especially in grade II and III. Visualization of the border between tumor tissue and normal brain tissue is extremely difficult, and complete resections are very rare when using conventional surgical method. The use of neuronavigation imaging data to demarcate the glioma boundaries, however, facilitates the implementation of total tumor resection.

Because of excellent tissue resolution, MRI (especially enhanced MRI) is often used as the input for neuronavigation during glioma resections. However, for grade II glioma, some grade III, and a few glioblastoma grade IV, MRI scans were not able to determine lesion boundaries or distinguish it from the surrounding edema. In the absence of apparent BBB damage, enhanced MRI was not able to show full the tumor extent, or the proliferation of heterogeneity within the tumor. In addition, the enhanced MRI may not show the real extent of the tumor invasion, so in some cases, MRI alone could not determine the surgical target. Our study revealed 9 cases in which high-grade gliomas showed mild or no enhancement on MRI, but high uptakes of FDG and MET on PET images. PET imaging, in particular, MET PET can clearly display the boundaries of glioma, the distinction between the tumor and surrounding edema, and the proliferation of different tumor areas [32, 34]. The data to determine the target for the application of PET stereotactic biopsy and stereotactic radiation therapy, confirm its high sensitivity and specificity [36-38]. The new PET/CT technique has significantly improved the precision of PET and combines the advantages of structural and functional imaging [39]. Combined with a neuronavigation system, PET could provide more comprehensive and precise imaging data to help more completely remove the tumor [40]. The project graphic workstation of our VectorVision®2 neuronavigation system could fuse the PET and MR or CT images.

We used the PET neuronavigation system to guide the surgery in twelve patients with glioma which had been difficult to confirm by routine CT and MR imaging. In particular, the actual tumor margin was undefined, and tumor and edema were not distinguished. In contrast, PET clearly identified the extent and invasiveness of the tumors, and provided the reliable data needed for neuronavigation-guided excision. In our study, grade II gliomas could not be distinguished from the normal brain tissue by visual inspection, and the boundary was not visible in the resected specimen. These operations were then continued using PET neuronavigation guidance. The degree of proliferation in different parts of some high grade gliomas could not be distinguished using MRI. In contrast, PET demonstrated distinctly both the tumor extent and the degree of proliferation in the various areas by the different uptakes of FDG and MET. Histological examination of the specimens showed that PET neuronavigation provided reliable distinction between normal brain tissue and glioma, the uptake of PET tracers can indicate the degree of proliferation. MET was more effective for this purpose than FDG [41].

## 6. Conclusion

PET imaging can fully reflect the tumor metabolic status, useful to preoperative assessment of brain glioma, and provide a new assistant for navigation of glioma surgery, especially when conventional imaging is difficult to determine the degree of malignancy and the extent of glioma. In addition, under the navigation, samples taken from different metabolic region, are profound to study on the biological characteristics of glioma.

## 7. References

- [1] Paulus W, Peiffer J. Intratumoral histologic heterogeneity of gliomas. A quantitative study. *Cancer* 64:442-447, 1989

- [2] Singhal T, Narayanan TK, Jain V, Mukherjee J, Mantil J. 11C-L-methionine positron emission tomography in the clinical management of cerebral gliomas. *Mol Imaging Biol* 10:1-18, 2008
- [3] Pirotte B, Goldman S, Dewitte O, Massager N, Wikler D, Lefranc F, Ben Taib NO, Rorive S, David P, Brotchi J, Levivier M. Integrated positron emission tomography and magnetic resonance imaging-guided resection of brain tumors: a report of 103 consecutive procedures. *J Neurosurg* 104:238-253, 2006
- [4] Tovi M, Lilja A, Bergstrom M, Ericsson A, Bergstrom K, Hartman M. Delineation of gliomas with magnetic resonance imaging using Gd-DTPA in comparison with computed tomography and positron emission tomography. *Acta Radiol* 31:417-429, 1990
- [5] Braun V, Dempf S, Weller R, Reske SN, Schachenmayr W, Richter HP. Cranial neuronavigation with direct integration of (11)C methionine positron emission tomography (PET) data—results of a pilot study in 32 surgical cases. *Acta Neurochir (Wien)* 144:777-782 discussion 782, 2002
- [6] Kracht LW, Miletic H, Busch S, Jacobs AH, Voges J, Hoevels M, Klein JC, Herholz K, Heiss WD. Delineation of brain tumor extent with [11C]L-methionine positron emission tomography: local comparison with stereotactic histopathology. *Clin Cancer Res* 10:7163-7170, 2004
- [7] Kaschten B, Stevenaert A, Sadzot B, Deprez M, Degueldre C, Del Fiore G, Luxen A, Reznik M. Preoperative evaluation of 54 gliomas by PET with fluorine-18-fluorodeoxyglucose and/or carbon-11-methionine. *J Nucl Med* 39:778-785, 1998
- [8] Alavi JB, Alavi A, Chawluk J, Kushner M, Powe J, Hickey W, Reivich M. Positron emission tomography in patients with glioma. A predictor of prognosis. *Cancer* 62:1074-1078, 1988
- [9] Borbely K, Nyary I, Toth M, Ericson K, Gulyas B. Optimization of semi-quantification in metabolic PET studies with 18F-fluorodeoxyglucose and 11C-methionine in the determination of malignancy of gliomas. *J Neurol Sci* 246:85-94, 2006
- [10] Goldman S, Levivier M, Pirotte B, Brucher JM, Wikler D, Damhaut P, Stanus E, Brotchi J, Hildebrand J. Regional glucose metabolism and histopathology of gliomas. A study based on positron emission tomography-guided stereotactic biopsy. *Cancer* 78:1098-1106, 1996
- [11] Ogawa T, Inugami A, Hatazawa J, Kanno I, Murakami M, Yasui N, Mineura K, Uemura K. Clinical positron emission tomography for brain tumors: comparison of fludeoxyglucose F18 and L-methyl-11C-methionine. *AJNR Am J Neuroradiol* 17:345-353, 1996
- [12] Padma MV, Said S, Jacobs M, Hwang DR, Dunigan K, Satter M, Christian B, Ruppert J, Bernstein T, Kraus G, Mantil JC. Prediction of pathology and survival by FDG PET in gliomas. *J Neurooncol* 64:227-237, 2003
- [13] Benard F, Romsa J, Hustinx R. Imaging gliomas with positron emission tomography and single-photon emission computed tomography. *Semin Nucl Med* 33:148-162, 2003
- [14] Chen W. Clinical applications of PET in brain tumors. *J Nucl Med* 48:1468-1481, 2007

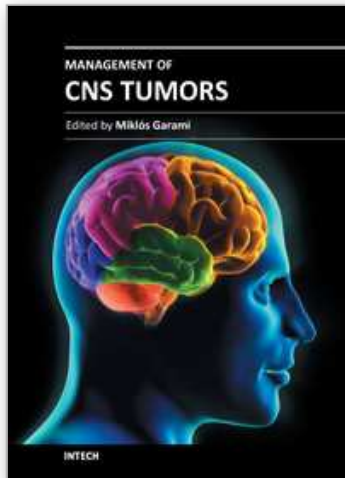
- [15] Kubota K. From tumor biology to clinical Pet: a review of positron emission tomography (PET) in oncology. *Ann Nucl Med* 15:471-486, 2001
- [16] Delbeke D, Meyerowitz C, Lapidus RL, Maciunas RJ, Jennings MT, Moots PL, Kessler RM. Optimal cutoff levels of F-18 fluorodeoxyglucose uptake in the differentiation of low-grade from high-grade brain tumors with PET. *Radiology* 195:47-52, 1995
- [17] Kato T, Shinoda J, Oka N, Miwa K, Nakayama N, Yano H, Maruyama T, Muragaki Y, Iwama T. Analysis of <sup>11</sup>Cmethionine uptake in low-grade gliomas and correlation with proliferative activity. *AJNR Am J Neuroradiol* 29:1867-1871, 2008
- [18] Nojiri T, Nariai T, Aoyagi M, Senda M, Ishii K, Ishiwata K, Ohno K. Contributions of biological tumor parameters to the incorporation rate of L: -[methyl-(<sup>11</sup>C)] methionine into astrocytomas and oligodendrogliomas. *J Neurooncol* 93:233-241, 2009
- [19] Wirtz CR, Albert FK, Schwaderer M, Heuer C, Staubert A, Tronnier VM, Knauth M, Kunze S: The benefit of neuronavigation for neurosurgery analyzed by its impact on glioblastoma surgery. *Neurol Res* 22: 354-360, 2000
- [20] Di Chiro G, DelaPaz RL, Brooks RA, et al. Glucose utilization of cerebral gliomas measured by [<sup>18</sup>F] fluorodeoxyglucose and positron emission tomography. *Neurology* 32:1323~1329, 1982
- [21] Patronas NJ, Brooks RA, DeLaPaz RL, Smith BH, Kornblith PL, Di Chiro G. Glycolytic rate (PET) and contrast enhancement (CT) in human cerebral gliomas. *AJNR Am J Neuroradiol* 4:533-535, 1983
- [22] Goldman S, Levivier M, Pirotte B, Brucher JM, Wikler D, Damhaut P, Dethy S, Brotchi J, Hildebrand J. Regional methionine and glucose uptake in high-grade gliomas: a comparative study on PETguided stereotactic biopsy. *J Nucl Med* 38:1459-1462, 1997
- [23] Bergstrom M, Collins VP, Ehrin E, Ericson K, Eriksson L, Greitz T, Halldin C, von Holst H, Langstrom B, Lilja A et al. Discrepancies in brain tumor extent as shown by computed tomography and positron emission tomography using [<sup>68</sup>Ga]EDTA, [<sup>11</sup>C]glucose, and [<sup>11</sup>C]methionine. *J Comput Assist Tomogr* 7:1062-1066, 1983
- [24] Mosskin M, Ericson K, Hindmarsh T, von Holst H, Collins VP, Bergstrom M, Eriksson L, Johnstrom P. Positron emission tomography compared with magnetic resonance imaging and computed tomography in supratentorial gliomas using multiple stereotactic biopsies as reference. *Acta Radiol* 30:225-232, 1989
- [25] Giammarile F, Cinotti LE, Jouvét A, Ramackers JM, Saint Pierre G, Thiesse P, Jouanneau E, Guyotat J, Pelissou-Guyotat I, Setiey A, Honnorat J, Le Bars D, Frappaz D. High and low grade oligodendrogliomas (ODG): correlation of amino-acid and glucose uptakes using PET and histological classifications. *J Neurooncol* 68:263-274, 2004
- [26] Utriainen M, Metsahonkala L, Salmi TT, et al. Metabolic characterization of childhood brain tumors: comparison of <sup>18</sup>F-fluorodeoxyglucose and <sup>11</sup>C-methionine positron emission tomography. *Cancer* 95: 1376~1386, 2002



- [27] Sadeghi N, Salmon I, Decaestecker C, Levivier M, Metens T, Wikler D, Denolin V, Rorive S, Massager N, Baleriaux D, Goldman S. Stereotactic comparison among cerebral blood volume, methionine uptake, and histopathology in brain glioma. *AJNR Am J Neuroradiol* 28:455-461, 2007
- [28] Kracht LW, Friese M, Herholz K, Schroeder R, Bauer B, Jacobs A, Heiss WD. Methyl-[11C]-l-methionine uptake as measured by positron emission tomography correlates to microvessel density in patients with glioma. *Eur J Nucl Med Mol Imaging* 30:868-873, 2003
- [29] Okita Y, Kinoshita M, Goto T, Kagawa N, Kishima H, Shimosegawa E, Hatazawa J, Hashimoto N, Yoshimine T. (11)Cmethionine uptake correlates with tumor cell density rather than with microvessel density in glioma: a stereotactic image-histology comparison. *Neuroimage* 49:2977-2982, 2010
- [30] Schaller B. Usefulness of positron emission tomography in diagnosis and treatment follow-up of brain tumors. *Neurobiol Dis* 15:437-448, 2004
- [31] Wei Chen. Clinical applications of PET in brain tumors. *J Nucl Med* 48:1468-1481, 2007
- [32] Wong TZ, van der Westhuizen GJ, Coleman RE. Positron emission tomography imaging of brain tumors. *Neuroimaging Clin N Am* 12(4):615-626, 2002
- [33] Gorska-Chrzastek M, Grzelak P, Bienkiewicz M, Tybor K, Zakrzewska E, Mikolajczak R, Stefanczyk L, Kusmierk J: Assessment of clinical usefulness of 131I alpha-methyl-tyrosine and fused SPECT/MRI imaging for diagnostics of recurrent cerebral gliomas. *Nucl Med Rev Cent East Eur* 7:135-141,2004
- [34] Chung JK, Kim YK, Kim SK, Lee YJ, Paek S, Yeo JS, Jeong JM, Lee DS, Jung HW, Lee MC: Usefulness of 11C-methionine PET in the evaluation of brain lesions that are hypo- or isometabolic on 18F-FDG PET. *Eur J Nucl Med Mol Imaging* 29:176-182, 2002
- [35] Floeth FW, Pauleit D, Wittsack HJ, Langen KJ, Reifenberger G, Hamacher K, Messing-Junger M, Zilles K, Weber F, Stummer W, Steiger HJ, Woebker G, Muller HW, Coenen H, Stabel M: Multimodal metabolic imaging of cerebral gliomas: positron emission tomography with [18F]fluoroethyl-L-tyrosine and magnetic resonance spectroscopy. *J Neurosurg* 102:318-327, 2005
- [36] Hara T, Kondo T, Hara T, Kosaka N: Use of 18F-choline and 11C-choline as contrast agents in positron emission tomography imaging-guided stereotactic biopsy sampling of gliomas. *J Neurosurg* 99:474-479, 2003
- [37] Lee JK, Liu RS, Shiang HR, Pan DH: Usefulness of semiquantitative FDG-PET in the prediction of brain tumor treatment response to gamma knife radiosurgery. *J Comput Assist Tomogr* 27:525-529, 2003
- [38] Levivier M, Massager N, Wikler D, Lorenzoni J, Ruiz S, Devriendt D, David P, Desmedt F, Simon S, Van Houtte P, Brotchi J, Goldman S: Use of stereotactic PET images in dosimetry planning of radiosurgery for brain tumors: clinical experience and proposed classification. *J Nucl Med* 45:1146-1154, 2004
- [39] von Schulthess GK. Positron emission tomography versus positron emission tomography/computed tomography: from "unclear" to "new-clear" medicine. *Mol Imaging Biol* 6:183-187, 2004



- [40] Nakajo K, Tatsumi M, Inoue A, Isohashi K, Higuchi I, Kato H, Imaizumi M, Enomoto T, Shimosegawa E, Kimura T, Hatazawa J: Diagnostic performance of fluorodeoxyglucose positron emission tomography/magnetic resonance imaging fusion images of gynecological malignant tumors: comparison with positron emission tomography/computed tomography. *Jpn J Radiol* 28(2):95-100, 2010
- [41] Yang S, Zhang C, Zhu T, Cai L, Gao S, Yue S, Wei W: Resection of gliomas using positron emission tomography/computed tomography neuronavigation. *Neurol Med Chir (Tokyo)* 47:397-401, 2007



## **Management of CNS Tumors**

Edited by Dr. Miklos Garami

ISBN 978-953-307-646-1

Hard cover, 464 pages

**Publisher** InTech

**Published online** 22, September, 2011

**Published in print edition** September, 2011

Management of CNS Tumors is a selected review of Central Nervous System (CNS) tumors with particular emphasis on pathological classification and complex treatment algorithms for each common tumor type. Additional detailed information is provided on selected CNS tumor associated disorders.

### **How to reference**

In order to correctly reference this scholarly work, feel free to copy and paste the following:

Yang Shuyuan, Zhang Chuan, Yue Shuyuan, Cai Li, Gao Shuo and Zhu Tao (2011). Preoperative Estimation and Resection of Gliomas Using Positron Emission Tomography/Computed Tomography Neuronavigation, Management of CNS Tumors, Dr. Miklos Garami (Ed.), ISBN: 978-953-307-646-1, InTech, Available from: <http://www.intechopen.com/books/management-of-cns-tumors/preoperative-estimation-and-resection-of-gliomas-using-positron-emission-tomography-computed-tomogra>

**INTECH**  
open science | open minds

### **InTech Europe**

University Campus STeP Ri  
Slavka Krautzeka 83/A  
51000 Rijeka, Croatia  
Phone: +385 (51) 770 447  
Fax: +385 (51) 686 166  
[www.intechopen.com](http://www.intechopen.com)

### **InTech China**

Unit 405, Office Block, Hotel Equatorial Shanghai  
No.65, Yan An Road (West), Shanghai, 200040, China  
中国上海市延安西路65号上海国际贵都大饭店办公楼405单元  
Phone: +86-21-62489820  
Fax: +86-21-62489821

© 2011 The Author(s). Licensee IntechOpen. This chapter is distributed under the terms of the [Creative Commons Attribution-NonCommercial-ShareAlike-3.0 License](#), which permits use, distribution and reproduction for non-commercial purposes, provided the original is properly cited and derivative works building on this content are distributed under the same license.

IntechOpen

IntechOpen